We are IntechOpen, the world's leading publisher of Open Access books Built by scientists, for scientists

4,800
Open access books available

122,000
International authors and editors

135M
Downloads

Our authors are among the

154
Countries delivered to

TOP 1%
most cited scientists

12.2%
Contributors from top 500 universities

CLARIVATE ANALYTICS BOOK CITATION INDEX INDEXED

WEB OF SCIENCE™

Selection of our books indexed in the Book Citation Index in Web of Science™ Core Collection (BKCI)

Interested in publishing with us?
Contact book.department@intechopen.com

Numbers displayed above are based on latest data collected.
For more information visit www.intechopen.com

18

An Active Contour and Kalman Filter for Underwater Target Tracking and Navigation

Muhammad Asif & Mohd Rizal Arshad
USM Robotics Research Group, Universiti Sains Malaysia
Malaysia

1. Introduction

The underwater survey and inspection are mandatory step for offshore industry and for mining organization from onshore-offshore structures installations to operations (Whitcomb, 2000). There are two main areas where underwater target tracking are presently employed for offshore and mining industry. First, sea floor survey and inspection and second is subsea installation, inspection and maintenance. This paper takes second area into account and AUV vision system is developed that can detect and track underwater installation such as oil or gas pipeline, and power or telecommunication cables for inspection and maintenance application. The usage of underwater installations has increased many folds. It is desirable to do routine inspection and maintenance to protect them from marine traffic, such as fishery and anchoring (Asakawa, et al., 2000). Detection and tracking of underwater pipeline in complex marine environment is fairly difficult task to achieve, due to the frequent presence of noise in a subsea surface. Noise is commonly introduced in underwater images by sporadic marine growth and dynamic lighting condition.

Traditionally, vigilances, inspections and maintenances of underwater man made structures are carried out by using the remotely operated vehicle (ROV) controlled from the mother ship by a trained operator (Whitcomb, 2000). The use of ROV's for underwater inspections are expensive and time consuming job. Furthermore controlling the ROV's from the surface by trained operators required continuous attention and concentration to keep the vehicle in the desired position and orientation. During long mission, this become a tedious task and highly prone to errors due to lack of attention and weariness. Moreover, tethering the vehicle limits both the operation range and the vehicle movements (Ortiz, 2002). The autonomous underwater vehicle's do not have such limitation and essentially present better capabilities to those of ROV's. AUV's have a wider range of operations as there is no physical link between the control station on the surface and the vehicle, as they carry their power supply onboard. The usage of AUV for underwater pipeline or cable inspection and maintenance become very popular area of research for mining and offshore industries (Griffiths & Birch 2000). During the last decade lots of efforts have been done for design and development of different AUV tracking system, to do routine inspection and maintenance for underwater installation (Asif and Arshad 2006). Conventionally, the literatures on underwater pipeline or cable tracking can be categorized according to the sensors used for detection and tracking. There are mainly three types of sensors which used for that purpose. The first two types of sensors are the sonar and the pair of magnetometers (Petillot, et al.,

Source: Mobile Robots Towards New Applications, ISBN 3-86611-314-5, Edited by Aleksandar Lazinica, pp. 784, ARS/plV, Germany, December 2006

2002; Evans, et al., 2003; Balasuriya & Ura 1999). These sensors provide effective tracking and successfully used in various tracking system. However, the problems with sensing devices are the power consumptions and the size of the devices itself. Furthermore, the measurements obtained using these sensors are extremely sensitive to noise. The third and most commonly used sensor for detection and inspection is the optical sensor or vision systems. The video camera mounted on a vehicle provides lots of information that can be examined by on board vision processing unit for effective path planning and navigations. Video camera is a high resolution sensor and is invaluable in situation required accurate measurements at short ranges. Generally, detection and tracking of an object in the natural marine environments using vision system presents several challenges (Ortiz, 2002). Due to the properties of ocean medium, optical waves are rapidly attenuated. Back scattering caused by marine snow, which are the presence of floating organic or inorganic particles in water which reflect light and degrades the visibility conditions.

Recently, several approaches to underwater pipeline tracking have purposed utilizing different characteristics such as 3D or 2D underwater pipeline or cable models (Balasuriya & Ura 1999; Foresti, 2001) and computational methods like template matching, Hough transform, neural network, standard or extended Kalman filter (Foresti, 2001). Conservatively, underwater tracking systems either based on feature based technique or they used underwater pipeline or cable model for detection and tracking in an image sequences. In feature based technique, tracking is performed by using the low level features such as pipeline boundary edges (Matsumoto & Ito 2002; Balasuriya, et al., 1997; Zanoli & Zingretti 1998). However, this technique may fail in case of occlusion due to growth of underwater plants or due to mud or sand on underwater pipeline or cable. On the other hand, model based approach based on prior knowledge or model of underwater pipeline such as straight line or structure of the underwater pipeline or cable (Balasuriya & Ura 1999; Foresti, 2001). The features extracted using the various image processing technique are matched with prior model. This prior model can be seen as a regularization term in measurement process. In this way model based method is robust against noise and missing data due to occlusion.

This paper purpose a model based approach to detect and track underwater pipeline in complex marine environments. The object of this research paper is to design and implement a vision guidance system for autonomous underwater pipeline tracking and navigation. The purposed vision system use unconventional gray scale conversion technique to enhance the image and then Perona Malik filter is used to reduce the noise effect and enhance the features of underwater pipeline. To detect the pipeline boundary in an image, Hough transform is used. After detecting the pipeline in an image, parameterized curve is used to represent the underwater pipeline and for feature extraction. Based on extracted feature, curve fitting is used to measure the current pose and orientation of underwater pipeline. In order to track the underwater pipeline over time in an image sequence, the pipeline tracking problem is formulated in terms of shape space model. Shape space model is a mathematical relation used for describing the state of underwater pipeline or cable. To estimate the state of underwater pipeline over time Kalman filtering is used.

The rest of paper is organized as follows: section 2 will presents the various image processing techniques that used for object detection in marine environments. Section 3 will discuss the methods for underwater pipeline modeling and shape space transformation. Section 4 will explain the feature extraction method and curve fitting technique. Section 5 will discuss the pose and orientation measurements for autonomous navigation. Section 6

will presents the dynamic modeling technique and Kalman filtering method for underwater pipeline tracking. Section 7 will discuss the results obtained by testing the purposed system on real underwater images and finally section 8 will end the paper with conclusion and future works.

2. Image processing

After the exploration of potential of vision sensor most autonomous vehicles now used onboard vision sensor for control and navigation. It can provide measurement relative to local objects. However vision sensor required special image processing techniques to detect object and surrounding environments in image or in image sequences. The image processing techniques implemented in this project are outlined in Fig. 1. The brief discussions on these techniques are followed.

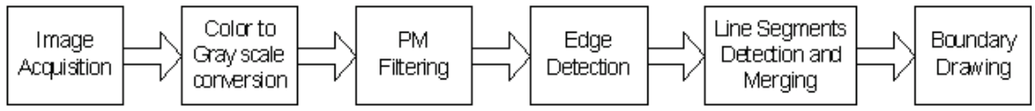

Fig. 1. Flow diagram for image processing.

2.1 Color to gray scale conversion

Conventionally the AUV is equipped with the color CCD camera to perform variety of task. The images acquired from the camera are in 24 bit RGB (Red, Green, and Blue) format. Colors are very important feature for any visual tracking system. However as the underwater installation gets older, corrosion, marine flora, and mud on underwater cables or pipeline modify this feature. So, as a first step of image analysis the images acquired by the onboard video camera are broken down to 8 bit values. There are several methods used to convert an RGB images into the grayscale, such as mean grayscale conversion, NTSC television standard and Intel image processing library formula. These types of conversion are suitable for several other applications such as television broadcasts and image editing and not very important for autonomous application. With this in mind different RGB channels are analyzed separately to enhance the images and extract boundary information of underwater pipeline effectively. Fig. 2 shows the individual analysis for red, green and blue channel. After doing series of experiments on real underwater images it found that the result of the red channel is well suited compare to green and blue channels. On the basis of these analyses only red channel is use for further processing.

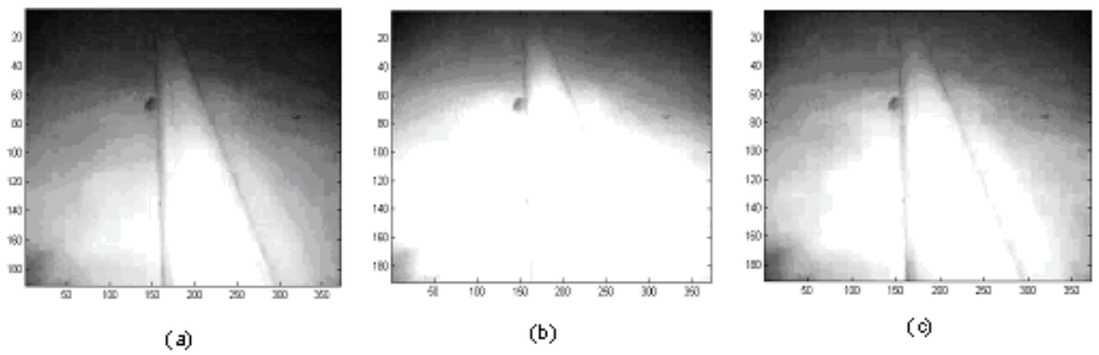

Fig. 2. Result of converting color image into gray image by extracting only the (a) Red, (b) Green and (c) Blue channel.

2.2 Image filtering

After converting image into the grayscale the next step is the image filtering. Due to the dynamic nature of lighting in the marine environment, images are often corrupted by noise. The existence of noise in an image affects the feature extraction step. As noise results in false edges being detected that may not exist and should not exist in the representation of the feature in the image. To overcome this problem, noise across the image is minimized by implementing smoothing or filtering operation Conventional smoothing techniques, like Gaussian, etc. are isotropic in nature and smooth the whole image in a similar fashion in all direction. Therefore while achieving the desired minimization of noise and variation across the image, the edges of the object in an image can loose contrast with the background. Further they also lead to the loss of the location of the actual boundaries. To cope up with this problem and to improve the image quality, the Perona-Malik (PM) filter (Perona & Malik 1990) has been selected for image filtering. The PM filter is anisotropic filter that retains the much needed edges information which is essential in detecting the pipeline boundary edges. It also improves the quality of the edge map obtains after edge detection, as edges are no longer produced around the noisy pixel regions. In Perona Malik filter, initial image I is modified using the anisotropic diffusion equation shown in (1).

$$\partial I_t = div(g(|\nabla I|)\nabla I) \tag{1}$$

where I is the original image, ∂I_t is the partial derivative of I with respect to diffusion time t, 'div' denotes the divergence operator, $|\nabla I|$ is the gradient magnitude of I and $g|\nabla I|$ is the diffusion coefficient diffusivity. The $g(x)$ is a nonnegative monotonically decreasing function with $g(0)=1$ and tend to zero at infinity so that the diffusion process will take place only in the interior. It will not affect the edges where the magnitude of the gradient is sufficiently large. The diffusivity function purposed by (Weickert, 2000) is used in this project as in (2)

$$g(\nabla I) = \begin{cases} 1 & if \quad |\nabla I_G| = 0 \\ 1 - \exp\left(\dfrac{-3.15}{(\nabla I/K)^2}\right) & if \quad |\nabla I_G| > 0 \end{cases} \tag{2}$$

where K is the threshold level for removing noise. The value of K plays very important role for smoothing the image without affecting the object edges and must be evaluated using the experimentation. This diffusivity function performs better in preserving/enhancing edges. To implement (1) a finite based approach is used, because it is comparatively straightforward to implement for digital images. Equation (1) then can be discretized using the four nearest neighbors (north, south, east and west) and the Laplacian operator are given by:

$$I_{i,j}^{n+1} = I_{i,j}^{n} + \lambda[C_N.\nabla_N I + C_S.\nabla_S I + C_W.\nabla_W I + C_E.\nabla_E I]_{i,j}^{n} \tag{3}$$

where

$$C_N = g(|\nabla_N I_{i,j}|$$
$$\nabla_N I_{i,j} = I_{i,j-1} - I_{i,j}$$
$$\nabla_N I_{i,j} = I_{i,j-1} - I_{i,j}$$

and similar for south, east, and west. Finally Fig. 3 shows the result of PM filter on real underwater images.

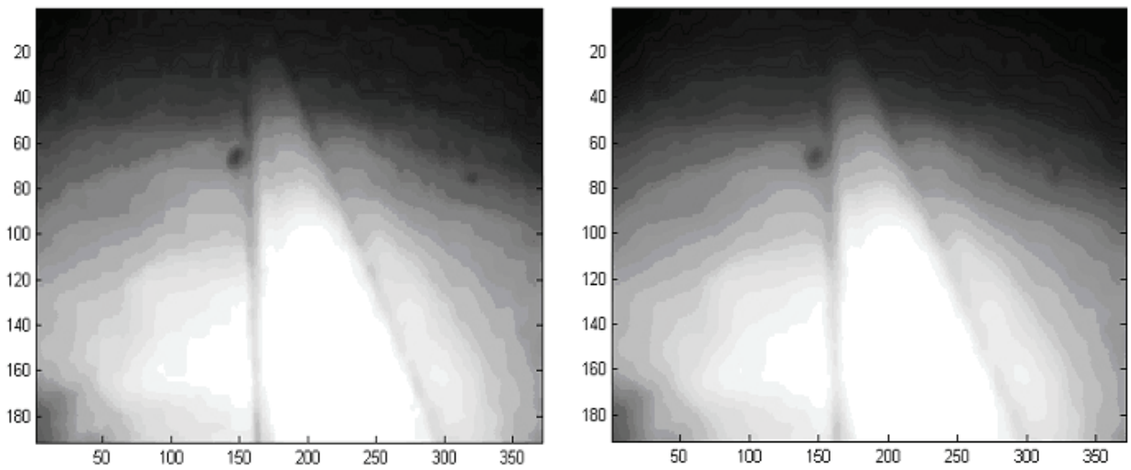

Fig. 3. Result of Perona-Malik filter with 10 and 20 iterations.

2.3 Pipeline detection

The next phase of image processing is the detection of pipeline boundary. Before detection of object boundary, edge detection is performed to convert gray scale image into the binary image. Since the image quality is already improved using the grayscale conversion and PM filtering, Sobel edge detection is used to avoid the computational burden.

Once image is converted into the binary, parameterized Hough transform is used to detect pipeline contour. The parametric equation of Hough transform is given below:

$$\rho = x\cos\theta + y\sin\theta \tag{4}$$

At first all edge points are transformed into the Hough space using (4). In order to avoid the computational burden and excessive memory usage of Hough transform, 1000 edge pixels are processed at a time. After transforming all the pixels in Hough space, peak detection is performed and the locations that contain the peaks are recorded. To avoid the quantization problem in Hough transform all the immediate neighborhood of the maximum found suppressed to zero. Once sets of candidate peaks are identified in the accumulator, start and end points of line segmentation associated with those peaks are identified next. If two line segments associated with the each other but separated by less then predefined gap threshold, are merge into a single line. Furthermore the lines that have both Hough parameters within the predefined threshold also merge in order to avoid multiple lines on same location. The start and the end points of line segments represent the outline of the underwater pipeline.

Due to noise and underwater conditions parts of the object boundary are detected. To draw a full boundary of the pipeline over an image a slight different approach is adopted. The first and last points of the line segment have been used to calculate the full boundary of the object using line equation. Once the slope of the line is computed from the line equation a Bresenham line algorithm, which is one of the oldest algorithms in computer graphics is used to construct a noise free boundary of the object. Bresenham line algorithm have few advantages, first it is relatively faster and simple to implement and it is robust if part of the pipeline is not visible or occluded. Fig. 4 shows the result of Hough transform and Bresenham line algorithm on underwater image.

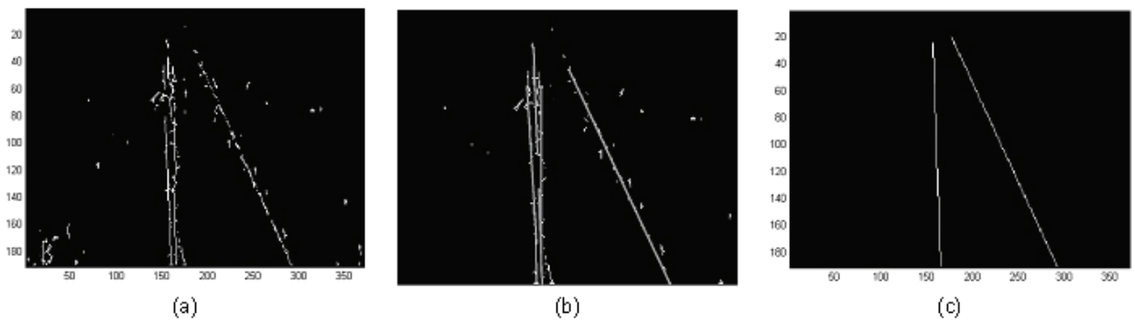

Fig. 4. Results of a) Edge image, b) Line segments detection using Hough Transform and c) Final image using Bresenham line Algorithm.

3. Underwater pipeline Model

After detecting the underwater pipeline in an image, the next phase is the design of deformable template that represents the perspective view of underwater pipeline boundaries. The deformable template uses a prior shape model that can be seen as a regularization term in the fitting process. To model the underwater pipeline in this work, second order non-uniform B-spline curve with six control points is used. The first three control points use to define the left boundary, while the last three control points are use to define right boundary of the pipeline as shown in Fig 5. The interval of the B-spline function is [0, 2] and the knot multiplicity on intervals are $k_0=k_1=k_2=0$, $k_3=k_4=k_5=k_6=k_7=k_8=1$ and $k_9=k_{10}=k_{11}=2$. The boundary contour $c(s) = (x(s), y(s))$ is then represented using a B-spline function is given below:

$$x(s) = \sum_{i=0}^{5} \mathbf{B}_i(s)\mathbf{Q}_x \qquad 0 \le s \le 2 \tag{5}$$

where $\mathbf{Q}_x = \begin{bmatrix} q_{-1}^x & q_0^x & q_1^x & q_2^x & q_3^x & q_4^x \end{bmatrix}^T$, and $\mathbf{B}(s) = (B_0(s),\ldots,B_5(s))$ and similarly for $y(s)$. The contour $c(s)$ of the pipeline boundary is also represented by a vector $\mathbf{Q}$ with the B-spline basis $U(s)$, so that:

$$c(s) = U(s)\mathbf{Q} \qquad \text{for } 0 \le s \le 2$$

where

$$U(s) = I_2 \otimes \mathbf{B}(s)^T = \begin{pmatrix} \mathbf{B}(s)^T & \mathbf{0} \\ \mathbf{0} & \mathbf{B}(s)^T \end{pmatrix} \tag{6}$$

and $\mathbf{Q} = (\mathbf{Q}^x \quad \mathbf{Q}^y)^T$. The I_2 denotes the 2x2 matrix, $\otimes$ is the Kronecker product and $\mathbf{Q}$ is the x-y coordinate of the B-spline curve. The matrix representation of the computed spline function is given in (7) and (8).

$$x_1(s) = \begin{pmatrix} 1 & s & s^2 \end{pmatrix} M_0 \begin{pmatrix} q_{-1}^x & q_0^x & q_1^x & q_2^x & q_3^x & q_4^x \end{pmatrix}^T \tag{7}$$

$$x_2(s) = \begin{pmatrix} 1 & s & s^2 \end{pmatrix} M_1 \begin{pmatrix} q_{-1}^x & q_0^x & q_1^x & q_2^x & q_3^x & q_4^x \end{pmatrix}^T \tag{8}$$

and similarly for $y(s)$. M_0 and M_1 are the span zero and span one matrix respectively as shown below:

$$M_0 = \begin{bmatrix} 1 & 0 & 0 & 0 & 0 & 0 \\ -2 & 2 & 0 & 0 & 0 & 0 \\ 1 & -2 & 1 & 0 & 0 & 0 \end{bmatrix}$$

and

$$M_1 = \begin{bmatrix} 0 & 0 & 0 & 1 & 0 & 0 \\ 0 & 0 & 0 & -2 & 2 & 0 \\ 0 & 0 & 0 & 1 & -2 & 1 \end{bmatrix}$$

The developed B-spline function provides convenient framework to track underwater pipeline in an image sequence over simple polynomial function or line function. The main disadvantage of the line or polynomial function is no local control. Since the features of underwater pipeline are random and small variation in any edge location will case big change in the orientation of line function or in polynomial function. Moreover these functions are not suitable to track flexible underwater installations, such as fiber optic cables. The main advantage of the designed underwater pipeline model is the local control because variation in features location only effect on a part of curve instead of whole curve and can track rigid and non-rigid installation without any modification.

The B-spline model used in this project has six control points. These six control points give 12 degree of freedom. It allows the arbitrary deformation of the contour, which does not happen for any real object. It is desirable to restrict the displacement of this control points to a lower dimensional space. It is assumed that the variation of pipeline boundaries in an image is linear and described by a shape space planar affine transformation. Affine shape space has 6 degrees of freedom, gives perspective effects and can handle translation and rotation. Affine shape space can be viewed as the class of all linear transformation that can be applied to a template curve $c_0(s)$ as in (9)

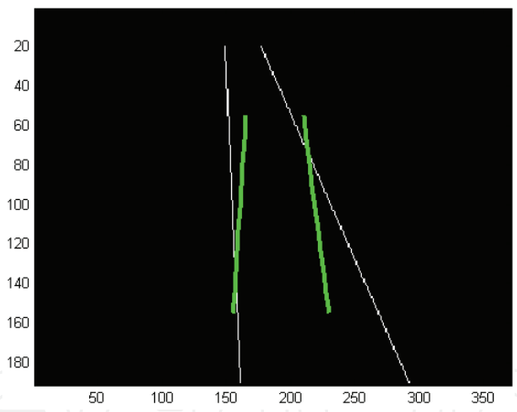

Fig. 5. B-spline contour that represents left and right boundaries of underwater pipeline, posted on underwater pipeline image.

$$c(s) = u + Mc_0(s) \tag{9}$$

where u is a two dimensional translation vector, and M is a 2x2 matrix which corresponds to remaining four affine motion. The affine space can be represented in a shape space (Blake & Israd 1998) with template $\mathbf{Q}_0$ and shape vector $\mathbf{X}$. A shape space is a linear mapping of a "shape-space vector" $\mathbf{X}$ to a spline vector $\mathbf{Q}$ as in (10)

$$\mathbf{Q} = W\mathbf{X} + \mathbf{Q}_0 \tag{10}$$

where W is $N_\mathbf{Q}$ by $N_\mathbf{X}$ shape matrix, $\mathbf{X}$ is a shape vector $\mathbf{X} \in S$, S is the set of all possible configuration of state and $N_\mathbf{Q}$ and $N_\mathbf{X}$ are the dimensions of spline vector and shape vector

respectively. **X** also called state vector because it represent the current state of the underwater object and $\mathbf{Q}_0$ is a template curve. The matrix W and shape space vector **X** are described as:

$$W = \begin{bmatrix} 1 & 0 & \mathbf{Q}_0^x & 0 & 0 & \mathbf{Q}_0^y \\ 0 & 1 & 0 & \mathbf{Q}_0^y & \mathbf{Q}_0^x & 0 \end{bmatrix}$$

$$\mathbf{X} = [d_1 \;\; d_2 \;\; A_{11} - 1 \;\; A_{22} - 1 \;\; A_{21} \;\; A_{12}]$$

The first two column of the shape matrix W represents the two dimensional (2D) translation and the remaining four columns comprise one rotation and three deformations (horizontal, vertical and diagonal). The dimension of the shape space N_x is usually small compared to the size of the spline vector N_Q. However the underwater pipeline or cable tracking required only 2 degree of freedom such as translation and rotation of the pipeline with respect to the center of the image plane and it is necessary to further reduce the degree of freedom of shape space. The further reduction of the shape space is achieved by using the Principle component analysis (PCA) which is commonly used to construct a shape space that is larger then necessary (Cootes, et al., 1995). In order to model the shape variation in a lower dimension L_2-norm PCA (Blake & Israd 1998) is used. L_2-norm PCA works satisfactorily compare to classical PCA as a mean of spline based curve representation. To measure the shape variations, various characteristic poses of underwater pipeline are taken as a training sets $\{\mathbf{X}_k, k=1,\ldots,M\}$. With the help of these training sets a mean and the covariance matrix are calculated using the (11) and (12).

$$\overline{\mathbf{X}} = \frac{1}{M}\sum_{k=1}^{M}\mathbf{X}_k \tag{11}$$

and

$$\overline{P} = \frac{1}{M}\sum_{k=1}^{M}(\mathbf{X}_k - \overline{\mathbf{X}})(\mathbf{X}_k - \overline{\mathbf{X}})^T \tag{12}$$

After that eigenvector and eigenvalues are computed with the multiple of covariance matrix $\overline{P}$ and the spare of the B-spline function H as shown in (13). This spare provides the invariance of the re-parameterization which is very important factor for measuring the difference between two spline based curve.

$$H = \begin{pmatrix} 1 & 0 \\ 0 & 1 \end{pmatrix} \otimes \frac{1}{L}\int_0^L \mathbf{B}(s)\mathbf{B}(s)^T ds \tag{13}$$

Once eigenvectors are computed in descending order of eigenvalues, W'' has been constructed next.

$$W'' = (v_1, \cdots, v_{N'x}) \tag{14}$$

where v represents eigenvectors. The parameters $\mathbf{Q}_0'$ and W′ of the shape subspace are given below:

$$\mathbf{Q}_0' = W\overline{\mathbf{X}} + \mathbf{Q}_0 \tag{15}$$

$$W' = WW'' \tag{16}$$

This compression reduced the shape space significantly, which is very important for visual servo application. Further, it also reduced the processing time as the matrix dimensional also reduced.

4. Feature extraction and curve fitting

Given an image containing the target, the measurement process consists of casting normals $\hat{n}(s)$ (called measurement line) at pre-specified points around the initial or current estimated contour as shown in Fig 6a. To extract the feature curve in the image, one dimensional feature detector is applied along each measurement line. The feature detector is simply a scanner that scans for intensity variation on the binary image obtained after Hough transform and Bresenham line algorithm. The measurement lines are unit normal vectors and the slopes of these normals are computed by differentiating the span zero B-spline function as shown in (17).

$$x_1'(s) = \begin{pmatrix} 0 & 1 & 2s \end{pmatrix} M_0 \begin{pmatrix} q_{-1}^x & q_0^x & q_1^x & q_2^x & q_3^x & q_4^x \end{pmatrix}^T \tag{17a}$$

and

$$y_1'(s) = \begin{pmatrix} 0 & 1 & 2s \end{pmatrix} M_0 \begin{pmatrix} q_{-1}^y & q_0^y & q_1^y & q_2^y & q_3^y & q_4^y \end{pmatrix}^T \tag{17b}$$

and similarly for span one B-spline function. The distance from a feature to the contour is called the innovation of the feature and is given in (22). The images obtained after Hough transform and Bresenham line algorithm ideally gives one feature point (left and right boundary of the pipeline or cable) along the normal as shown in Fig 6b. However due to sporadic marine growth and dynamic underwater conditions, there may be no or more than one feature along the normal. It required some mechanism for evaluating the measurement and picking the correct feature point that used in subsequent calculations. This evaluation is done by using the innovation of the feature which is the distance between the estimated curve point and the feature curve point. If there are more features, the innovation that gives the minimum distance is selected and if the selected innovation is greater than the predefine value, the measurement is invalidated.

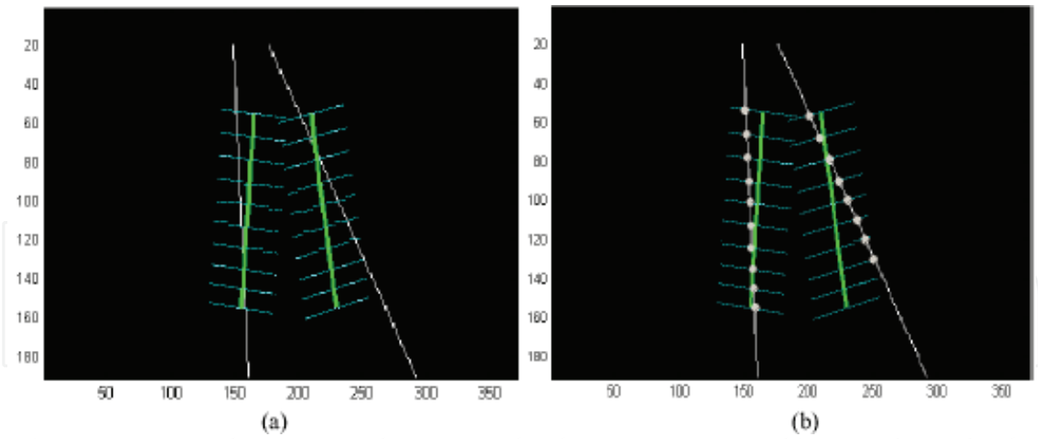

Fig. 6a) Measurement line on B-spline curve for feature extraction b) Dots show the feature extracted using the one-dimensional feature detector.

After extracting the feature points in an image, the next part of tracking algorithm is to use curve fitting technique to measure the current position and orientation of the underwater pipeline. If $c_f(s)$ expressed the image feature curve obtained using the one dimensional feature detector and $c_0(s)$ is a pattern curve than, the whole tracking is the estimate $c(s)$, a B-spline curve that is a deformation of $c_0(s)$ and that approximate $c_f(s)$. This approximation can be express as a minimization problem:

$$r = \arg\min \left\| c(s) - c_f(s) \right\|^2 \tag{17}$$

which is the square of the residual norm. Generally, measurements made from images are noisy due to dynamic nature of underwater environments and several other reasons. It is necessary to increase the tolerance for image noise. To overcome the effect of noise a mean contour shape and Tikhonov regularization are used to bias the fitted curve toward the mean shape c_m to the degree determined by regularization constant as shown in (18).

$$r = \arg\min \left(\Omega^2 \left\| c(s) - c_m(s) \right\|^2 + \left\| c(s) - c_f(s) \right\|^2 \right) \tag{18}$$

where $c_m(s)$ is the mean shape and Ω is the regularization parameter. If the regularization parameter is very large, the term $\left\| c(s) - c_f(s) \right\|$ is negligible to that of $\Omega^2 \left\| c(s) - c_m(s) \right\|$ in (18). With a large amount of regularization, the data and any noise on the data can be ignored effectively. On the other hand if Ω is small, the weighting placed on the solution semi norm is small and the value of the misfit at the solution become more important. Of course, if Ω is reduced to zero, the problem reduces to the least-square case as in (17), with it extreme sensitivity to noise on the data. Equation (19) shows the fitting equation in term of shape state vector **X**.

$$\min \mathbf{X} = \Omega^2 \left\| \mathbf{X} - \bar{\mathbf{X}} \right\|^2 + \left\| \mathbf{Q} - \mathbf{Q}_f \right\|^2 \text{ with } \mathbf{Q} = W\mathbf{X} + \mathbf{Q}_0 \tag{19}$$

To avoid the influence of position and orientation of the mean contour and from the features of other objects in the background in the regularization term, weight matrix L^s is introduced as in (20).

$$\min \mathbf{X} = \left\| \mathbf{X} - \bar{\mathbf{X}} \right\|^T L^s \left\| \mathbf{X} - \bar{\mathbf{X}} \right\| + \left\| \mathbf{Q} - \mathbf{Q}_f \right\|^2 \tag{20}$$

where $L^S = \Omega H$ and H is the spare of B-spline function as defined in (13). Since actual image processing is discrete, by using the definition given in (Blake & Israd 1998) the curve fitting problem is expressed in a discrete form as follows:

$$\min \mathbf{X} \left\| \mathbf{X} \text{-} \bar{\mathbf{X}} \right\|^T L^s \left\| \mathbf{X} \text{-} \bar{\mathbf{X}} \right\| + \sum_{i=1}^{N} \frac{1}{\sigma_i^2} \left(v_i - \mathbf{h}(s_i)^T [\mathbf{X} - \bar{\mathbf{X}}] \right)^2 \tag{21}$$

where v_i and $\mathbf{h}(s_i)^T$ are given in (22) and (23) respectively. Introducing the concept of information matrix S_i and information weight sum $\mathbf{Z}_i$ from the stochastic process, the algorithm for finding the best-fitting curve is summarized as follows:

- Select N regularly equal-spaced sample points $s=s_i$, $i=1,\ldots,N$, with inter-sample space h, along the entire curve $c(s)$ so that, in the case of an open curve $s_1=0$, $s_{i+1}=s_i+h$ and $s_N=L$.
- For each i, find the position of $c_f(s)$ by applying 1D feature detector along the normal line passing though $c(s)$ at $s=s_i$.
- Initialize $\mathbf{Z}_0 = 0, \quad S_0 = 0$

  Iterate, for $i=1,\ldots,N$

$$v_i = \left(c_f(s_i) - \bar{c}(s_i) \right) . \bar{\mathbf{n}}(s_i) \tag{22}$$

$$\mathbf{h}(s_i)^T = \bar{\mathbf{n}}(s_i)^T U(s_i) W \tag{23}$$

  if $|vi| < k$ then

$$S_i = S_{i-1} + \frac{1}{\sigma_i^2}\mathbf{h}(s_i)\mathbf{h}(s_i)^T \tag{24}$$

$$\mathbf{Z}_i = \mathbf{Z}_{i-1} + \frac{1}{\sigma_i^2}\mathbf{h}(s_i)v_i \tag{25}$$

Else

$$S_i = S_{i-1};\ \ \mathbf{Z}_i = \mathbf{Z}_{i-1}$$

where $n(s_i)$ is the normal unit vector of curve $\bar{c}(s)$ at $s=s_i$, $\sigma_i^2 = N_B$ and k is the length of the measurement line.

- The aggregated observation vector is $\mathbf{Z}=\mathbf{Z}_N$ with the associated statistical information $S=S_N$.
- The best-fitting curve is given in shape-space by:

$$\hat{\mathbf{X}} = \bar{\mathbf{X}} + (\bar{S} + S)^{-1}\mathbf{Z} \tag{26}$$

The term $|vi|<k$ is used for measurement validation as described earlier. S_i (information matrix) is a measurement of the weight of each intermediate estimate $\mathbf{X}$, $\mathbf{Z}_i$ (information weight sum) accumulates the influence of the mean shape c_m. The proof of correctness of the curve fitting algorithm can be found in (Blake & Israd 1998).

5. Pose and orientation measurement

After the shape vector, that represents the current state of underwater pipeline, is estimated, the goal is to guide the autonomous underwater vehicle in autonomously following the pipeline. It required some mechanism to relate the position and orientation of the underwater pipeline to the AUV. This mechanism is necessary for the AUV to keep the underwater pipeline within the field of view. The mean shape c_m of the underwater pipeline introduced in (18) is used as a reference location for the underwater pipeline in an image. The reference position of underwater pipeline in an image can be measure by averaging the control points of the mean shape as in (27).

$$\bar{A}_X = mean(\mathbf{Q}_m^x) \tag{27}$$

and

$$\bar{A}_y = mean(\mathbf{Q}_m^y)$$

This average actually presents the centroid of the control points which lies almost in the center of the image. This information is needed so that the AUV can effectively maintain the underwater pipeline in the center of the image acquired. The B-spline model developed to represent underwater pipeline in an image, is set fixed in y-direction so, the translation in y-direction is always zero and not required. The shape vector estimated in (26) is used to measure the current position of the control points using (10). The average of these control points gives the current position of underwater pipeline in an image as shown in (28)

$$A_X = mean(\mathbf{Q}^x) \tag{28}$$

The current distance of the pipeline in an image with respect to the reference can be measure by subtracting the reference position from the current position as shown in (29)

$$T_X = A_X - \bar{A}_X \tag{29}$$

It is obvious that the positive value of T_X refer the pipeline as is translated to the right, and the negative means that the pipeline is translating toward the left side. The value of T_X can then be used to generate a navigational command, in order to align an AUV over the pipeline, and keep the pipeline in the optimum filed of view. The location of the pipeline can be use to track an underwater pipeline in an image, however this is an ineffective method. It may possible that the AUV may be facing the wrong direction after aligning, and the tracking system must calculate the orientation of the pipeline for correct navigation. Once the autonomous underwater vehicle has aligned to the location of the pipeline, the tracking system will then instruct AUV to rotate itself in the calculated pipeline orientation and commence autonomous tracking.
Similar to the location measurement, at first the reference orientation of underwater pipeline is measured using the mean curve control points. As mentioned earlier, the perspective view of underwater pipeline is modeled using the left and right B-spline curve. The orientation of the left and right reference boundaries are given below:

$$\overline{R}_{L1} = \tan^{-1}\left(\frac{q_0^y - q_{-1}^y}{q_0^x - q_{-1}^x}\right),\ \overline{R}_{L2} = \tan^{-1}\left(\frac{q_0^y - q_1^y}{q_0^x - q_1^x}\right),\ \text{and}\ \overline{R}_{L3} = \tan^{-1}\left(\frac{q_{-1}^y - q_1^y}{q_{-1}^x - q_1^x}\right)$$

and

$$\overline{R}_{R1} = \tan^{-1}\left(\frac{q_2^y - q_3^y}{q_2^x - q_3^x}\right),\ \overline{R}_{R2} = \tan^{-1}\left(\frac{q_4^y - q_3^y}{q_4^x - q_3^x}\right),\ \text{and}\ \overline{R}_{R3} = \tan^{-1}\left(\frac{q_2^y - q_4^y}{q_2^x - q_4^x}\right)$$

where $\overline{R}_{L1}, \overline{R}_{L2}, \overline{R}_{L3}, \overline{R}_{R1}, \overline{R}_{R2},$ and $\overline{R}_{R3}$ are the angles between the left and right boundaries control points. These angles now use as reference angles to measure the pipeline variation. The orientation of the current estimated control points are measured in a similar fashion

$$R_{L1} = \tan^{-1}\left(\frac{q_0^y - q_{-1}^y}{q_0^x - q_{-1}^x}\right),\ R_{L2} = \tan^{-1}\left(\frac{q_0^y - q_1^y}{q_0^x - q_1^x}\right),\ \text{and}\ R_{L3} = \tan^{-1}\left(\frac{q_{-1}^y - q_1^y}{q_{-1}^x - q_1^x}\right)$$

and

$$R_{R1} = \tan^{-1}\left(\frac{q_2^y - q_3^y}{q_2^x - q_3^x}\right),\ R_{R2} = \tan^{-1}\left(\frac{q_4^y - q_3^y}{q_4^x - q_3^x}\right),\ \text{and}\ R_{R3} = \tan^{-1}\left(\frac{q_2^y - q_4^y}{q_2^x - q_4^x}\right)$$

After measuring the orientation of each current estimated control points, the Euclidean angle between the two corresponding control points are measured as shown below:

$$R_1 = R_{L1} - \overline{R}_{L1},\ R_2 = R_{L2} - \overline{R}_{L2}\ \text{and},\ R_3 = R_{L3} - \overline{R}_{L3}$$

$$R_4 = R_{R1} - \overline{R}_{R1},\ R_5 = R_{R2} - \overline{R}_{R2}\ \text{and},\ R_6 = R_{R3} - \overline{R}_{R3}$$

Once all the Euclidean angles have measured, the minimum Euclidean angle is selected as a rotation angle for the AUV.

$$R = \min(R_1, R_2, R_3, R_4, R_5, \text{ and } R_6)$$

After the translation and rotation of the underwater pipeline with respect to the mean curve are measured, the autonomous underwater vehicle has aligned and orientated itself in the direction of the pipeline. The AUV subsequently start moving in the direction of the underwater pipeline and begin autonomous navigation.

6. Dynamic tracking

Any tracking system required a model of how the system is expected to evolve or behave over time (MacCormick, 2000). In this work, second order auto-regressive process or ARP is used. An autoregressive process is a time series modeling strategy which takes into account the historical data to predict the current state value. The simplest autoregressive model is the linear model where the AUV is assumed to have a constant velocity model with respect to the object. It is best described by the following second order autoregressive model:

$$\mathbf{X}_t - \overline{\mathbf{X}} = A_2(\mathbf{X}_{t-2} - \overline{\mathbf{X}}) + A_1(\mathbf{X}_{t-1} - \overline{\mathbf{X}}) + B_0\mathbf{w}_k \tag{26}$$

where **w** is a random Gaussian noise with zero mean and unit standard deviation, **X** is the steady state mean and $\mathbf{X}_t$ is the position of object at time *t*. The matrices *A* and *B* are representing the deterministic and stochastic parameters respectively. These parameters are needed to be tuned appropriately for expected motion in order to obtain best tracking results. If β and *f* are expressed the damping rate and the frequency of oscillation of the harmonic motion respectively then according to the theory of control system they must set to zero for constant velocity model, so that the coefficients of the dynamic model are defined as:

$$A_1 = \begin{pmatrix} 2 & 0 & 0 \\ 0 & 2 & 0 \\ 0 & 0 & 2 \end{pmatrix} A_2 = \begin{pmatrix} -1 & 0 & 0 \\ 0 & -1 & 0 \\ 0 & 0 & -1 \end{pmatrix} B_0 = \begin{pmatrix} 3 & 0 & 0 \\ 0 & 3 & 0 \\ 0 & 0 & 3 \end{pmatrix} \tag{27}$$

where A_1 and A_2 are standard for all second order constant velocity model. The problem is the estimation of B_0 and it required a tuning from the experiment because it defines the standard deviation of the noise. Equation 26 can be simplified by defining:

$$\chi_t = \begin{pmatrix} \mathbf{X}_{t-1} \\ \mathbf{X}_t \end{pmatrix}, \tag{28}$$

and then (26) can be rewritten as:

$$\chi_t - \overline{\chi} = A(\chi_{t-1} - \overline{\chi}) + B\mathbf{w}_k \tag{29}$$

where

$$A = \begin{pmatrix} 0 & I \\ A_2 & A_1 \end{pmatrix}, \overline{\chi} = \begin{pmatrix} \overline{\mathbf{X}} \\ \overline{\mathbf{X}} \end{pmatrix} \text{ and } B = \begin{pmatrix} 0 \\ B_0 \end{pmatrix}$$

The second order state χ_t has a mean and covariance is given below:

$$\hat{\chi}_t = \varepsilon[\chi_t] \text{ and } \vec{P}_t = v[\chi_t]$$

A Kalman filter is design to merge the information from the predicted state and the best fitting curve obtain from (26). A complete one step cycle of tracking is given below:
1. Predict shape space vector χ_t using the dynamic model:

$$\tilde{\chi}_t - \overline{\chi} = A(\hat{\chi}_{t-1} - \overline{\chi}) \tag{30}$$

$$\tilde{\vec{P}}_t = A\tilde{\vec{P}}_{t-1}A^T + BB^T \tag{31}$$

2. Apply (22) to (26) to estimated best fitted state of object.
3. For each measurement the state estimation is update as follows:

$$\mathbf{K}_t = \tilde{\tilde{P}}_t \mathbf{H}^T \left(S_t \mathbf{H} \tilde{\tilde{P}}_t \mathbf{H}^T + I \right)^{-1} \tag{32}$$

$$\hat{\chi}_t = \tilde{\chi}_t + \mathbf{K}_t \mathbf{Z}_t \tag{33}$$

$$\ddot{P}_t = (I - \mathbf{K}_t S_t \mathbf{H}) \tilde{\tilde{P}}_t \tag{34}$$

and

$$\mathbf{H} = (0 \quad I) \tag{35}$$

The term $\mathbf{Z}_t$ and S_t are aggregated observation vector and associated statistical information respectively. If the measurement failed along the normal due to occlusion or multiple features so that $\mathbf{Z}_t = 0$ and $S_t = 0$, and the state of underwater pipeline is estimated without modification.

7. Results and Discussion

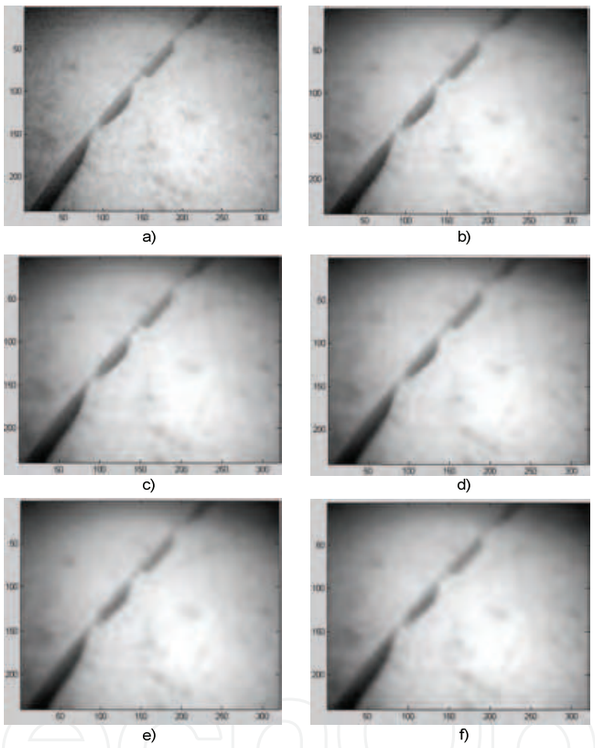

Fig. 7a Results of Perona-Malik filter with N=10 a) original image b) K = 5 c) K = 10 d) K = 15 e) K = 25 f) K = 40.

This section presents the results which were obtained by testing the proposed underwater pipeline tracking system using AUV real image sequences. As a first step of feature extraction, image filtering was performed to reduce the noise in the image sequence. The key parameters in the Perona-Malik filter are the threshold level for noise removing (K) and the number of iterations N. The noise threshold level (K) was analyzed with different values of K's with fix number of iterations. Fig. 7a and Fig. 7b show the effect of Perona Malik filter with varying values of K on synthetic and real images respectively. It is observed that the increasing the value of K also increase the smoothness of image while preserving the object boundary. The best results were obtained at K=15. Large value of K effectively reduces the noise in an image but they also smooth the object boundary and edge detection may fail to

detect. Based on these visual analysis the value K=15 was selected for further filtering process. The second important parameter in Perona Malik filter is the number of iterations. Much improved results can be obtained using the large number of iterations however, it also increase the computational time for filtering which is not at all required for robotic application. To achieve the optimal performance the number of iterations are fixed to N=10 only. Fig. 8 shows the comparison of edge detection results between the original and filtered underwater image sequences. The average number of edge filtering is approximately 770 pixels with K=15 and N=10 iterations. These reductions of edges significantly improve the results of feature detection.

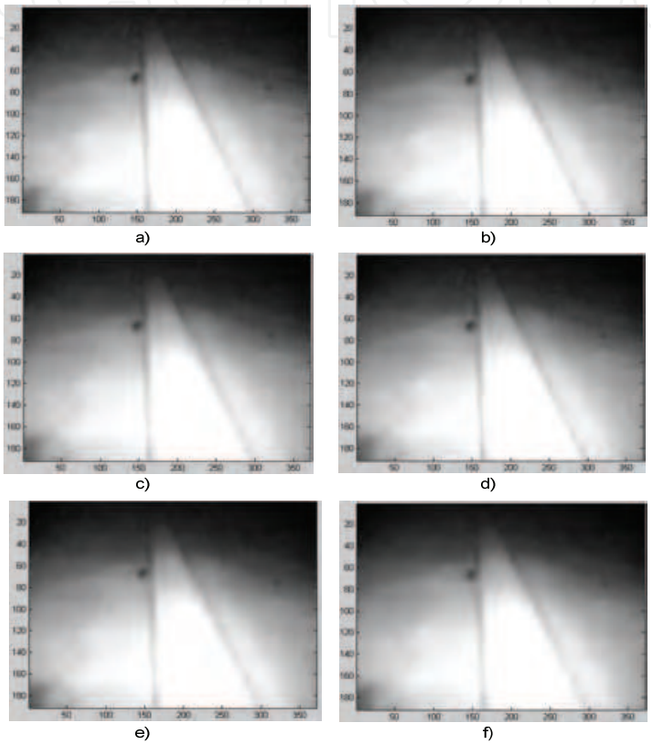

Fig. 7b. Results of Perona-Malik filter with N=10 a) original image b) K = 5 c) K = 10 d) K = 15 e) K= 25 f) K = 40.

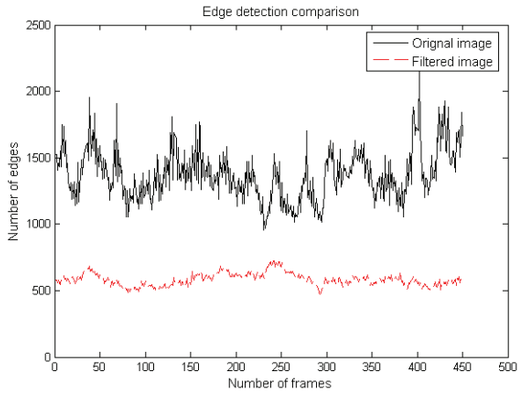

Fig. 8. Edge detection comparisons between original and filtered underwater image sequence.

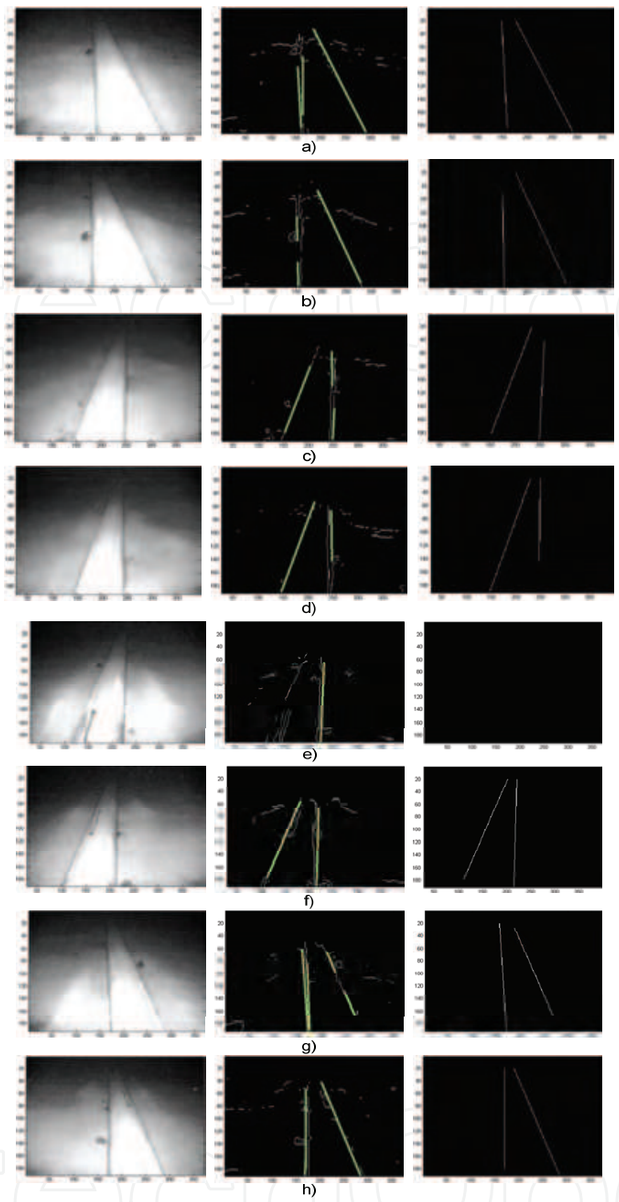

Fig. 9. Results of Hough transform and Bresenham line algorithm. First column original image, 2nd column results of Hough transform, and 3rd column is the results of Bresenham line algorithm.

Underwater pipeline detection	Performance	%
Correctly detected	419	93.11%
Not detected	31	6.88%

Table 1. Performance measurement for the underwater pipeline detection.

After filtering the image, the next part of the image processing involves the detection of the underwater pipeline in an image sequences using Hough transform. In order to perform the pipeline detection, the θ parameter was quantized into 180 levels and the ρ parameter was quantized using the root mean square value of total numbers of row and column of image frame. The gap threshold was set to 25 levels and the minimum segment length was 30

pixels. These values were obtained by a series of experiments on real underwater images. After detecting the pipeline segments in an image, Bresenham line used to draw the pipeline boundary. Fig. 9 shows the results of Hough transform and the Bresenham line algorithm on real underwater images. The Hough transform and Bresenham line algorithm successfully detect and draw the boundary of underwater pipeline. Table 1 displays some performance results calculated using a batch of 450 real images.

These results can be further improved upon, if the Hough parameter space is increased. Additionally canny edge detection can also be use to improve the accuracy of edge mapping. Although these amendments increase the probability of underwater pipeline detection, it may results in an increment of false detections and also increases computational time.

After detecting the pipeline in an image frame the next phase was the extraction of feature points from an image. In general, the accuracy and the performance of the tracking algorithm improve as the number of feature points, used in curve fitting stage increases. However, as the number of feature increases the computational load become heavier. There is an obvious trade-off between accuracy of the tracking algorithm and the computational time. To achieve the balance between performance and efficiency, 20 feature points were used. It was observed from the experimentation that, at least five feature points on either side are required for successful deformation of template contour to the image features. If there are fewer features then the state of the underwater pipeline was predicted without modification. Fig 10 depicted the underwater pipeline tracking results obtained using the Kalman tracking algorithm. Every 10^{th} frame of 4500 frames sequences was used to check the robustness and the accuracy of the tracking algorithm. The position and the orientation of the underwater pipeline boundary computed are summarized in the table 1. Fig 11 illustrates the predicted, updated and the actual position of the underwater pipeline. It is observed that the maximum absolute error in the translation is around 12 pixels which show the robustness of tracking algorithm. To solve the initial value problem of the Kalman filter, it has been assumed that when tracking is started pipeline is near the center of the image. In other words, mean shape $\bar{\mathbf{x}}$ and covariance $\bar{P}$ used as the initial value for $\mathbf{X}_{t0}=\bar{\mathbf{x}}$.

	Actual Position	Estimated Position	Error	Estimated Angle
Average	197.38	197.98	-0.60	0.34
Max	224.33	217.45	10.75	2.80
Min	179.54	171.30	-12.65	-0.99
Mode	193.77	-	3.46	-

Table 2. Summary of Kalman Tracking Results.

8. Conclusion

In this paper a robust vision based system for underwater pipeline tracking has been presented. The developed system successfully detects the pipeline and track in real image sequences. The algorithm has been implemented in Matlab environment and all test have been conducted on a 1.70 GHz Pentium IV machine executing Windows XP. The resolution of both synthetic and real image sequences is 200 x 370 pixels.

The B-spline contour deforms successfully, based on the features extracted with the series of image processing technique and the orientation and the position of the pipeline has been computed. The Kalman filter has been used to track the pipeline boundary in an image sequences. The system efficiently track the pipeline when it is fully or partially covered by the sand or marine flora and even in clustering situations.

To conform the validity of the purposed system many experiments conducted on real and synthetic underwater pipeline image sequences. The maximum error that has been achieved is less then 10 pixels which show the robustness of the purposed system. Since the purposed system implemented in Matlab so, it takes 1 sec to process each frame. In order to improve the processing time the system will be implemented in C++. Furthermore in the case of multiple pipelines and to achieve better performance particle filtering technique will be explored.

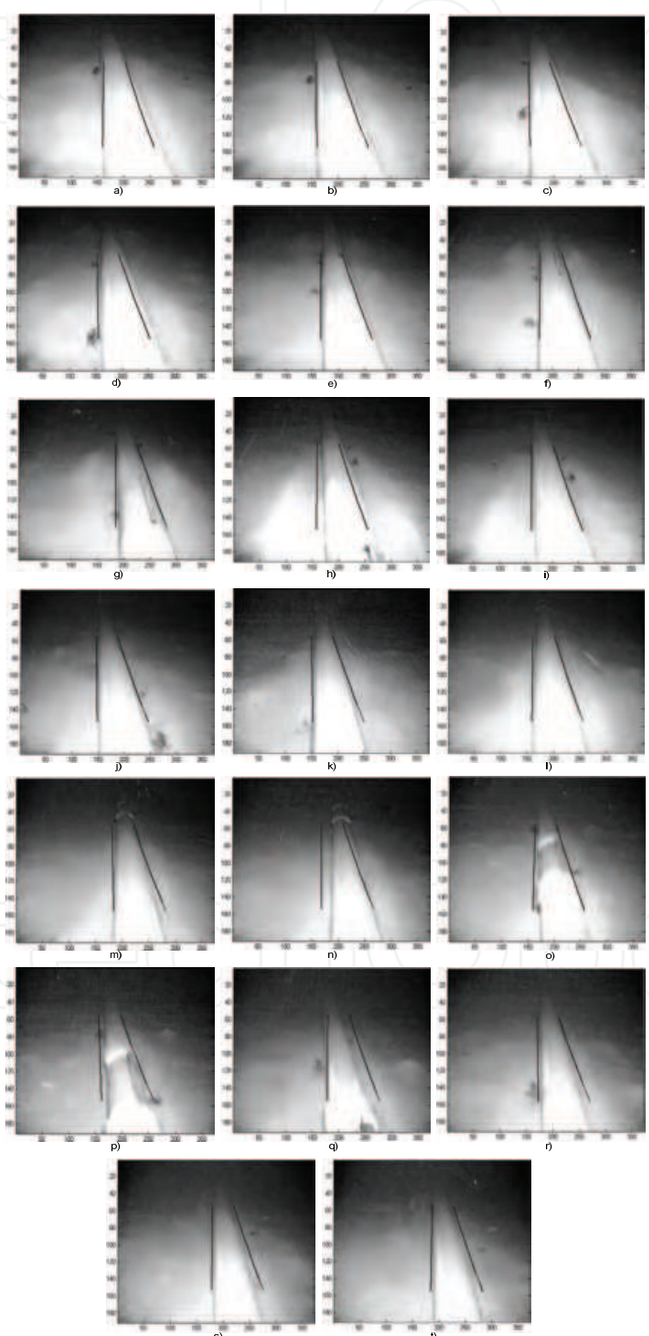

Fig. 10 Underwater pipeline tracking results with Kalman filter.

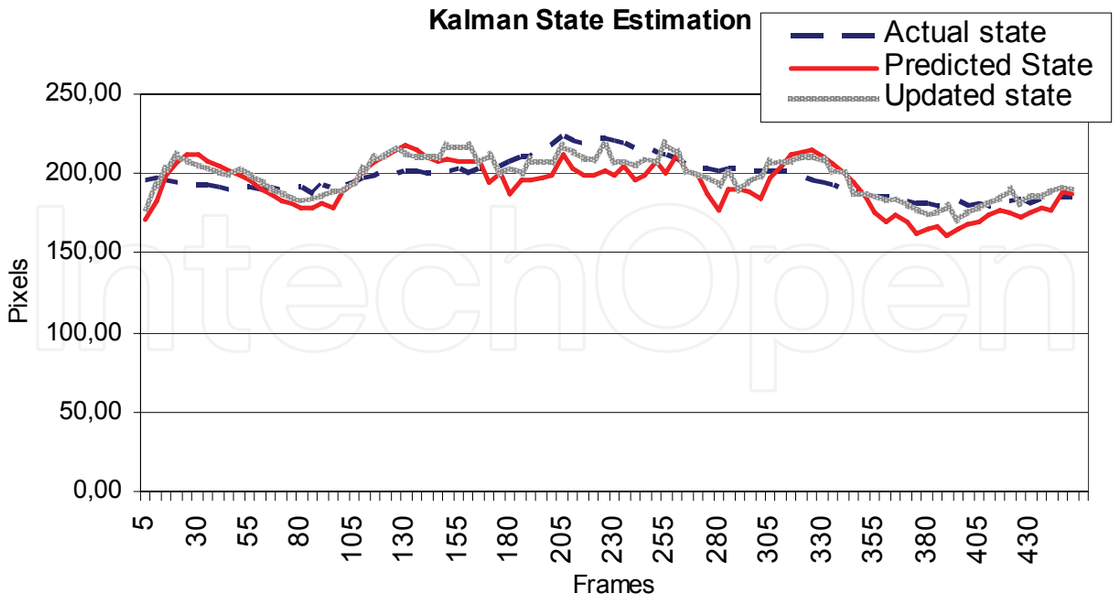

Fig. 11. Comparison of actual and predicted and updated position of underwater pipeline using the Kalman tracking algorithm.

9. References

Whitcomb, L.L. (2000). Underwater robotics: out of the research laboratory and into the field, *IEEE International Conference on Robotics and Automation, ICRA '00,* Vol.1, 24-28 April 2000, pp. 709 – 716.

Asakawa, K., Kojima, J., Kato, Y., Matsumoto, S. and Kato, N. (2000). Autonomous underwater vehicle AQUA EXPLORER 2 for inspection of underwater cables, *Proceedings of the 2000 International Symposium on Underwater Technology, 2000, UT 00*. 23-26 May 2000, pp. 242 – 247.

Ortiz, A., Simo, M., Oliver, G. (2002). A vision system for an underwater cable tracker, *Machine vision and application 2002*, Vol.13 (3), July 2002, pp. 129-140.

Griffiths, G. and Birch, K. (2000). Oceanographic surveys with a 50 hour endurance autonomous underwater vehicle, Proceeding of the Offshore Technology Conference, May 2000, Houston, TX.

Asif, M. and Arshad, M.R. (2006). Visual tracking system for underwater pipeline inspection and maintenance application, *First International Conference on Underwater System Technology, USYS06*. 18 – 20 July 2006, pp 70-75.

Cowls, S. and Jordan, S. (2002). The enhancement and verification of a pulse induction based buried pipe and cable survey system. *Oceans '02 MTS/IEEE.* Vol. 1, 29-31 Oct. 2002, pp. 508 – 511.

Petillot, Y.R., Reed, S.R. and Bell, J.M. (2002). Real time AUV pipeline detection and tracking using side scan sonar and multi-beam echo-sounder, *Oceans '02 MTS/IEEE.* Vol. 1, 29-31 Oct. 2002, pp. 217 - 222.

Evans, J., Petillot, Y., Redmond, P., Wilson, M. and Lane, D. (2003). AUTOTRACKER: AUV

embedded control architecture for autonomous pipeline and cable tracking, *OCEANS 2003, Proceedings,* Vol. 5, 22-26 Sept. 2003, pp. 2651 – 2658.

Balasuriya, A. & Ura, T. (1999) Multi-sensor fusion for autonomous underwater cable tracking, *Riding the Crest into the 21st Century OCEANS '99 MTS/IEEE,* Vol. 1, 13-16 Sept. 1999, pp. 209 – 215.

Foresti, G.L. (2001). Visual inspection of sea bottom structures by an autonomous underwater vehicle Systems, *IEEE Transactions on Man and Cybernetics, Part B*, Vol. 31 (5), Oct. 2001, pp. 691 – 705.

Matsumoto, S. & Ito, Y. (1997). Real-time vision-based tracking of submarine-cables for AUV/ROV, *MTS/IEEE Conference Proceedings of OCEANS '95, 'Challenges of Our Changing Global Environment,* Vol. 3, 9-12 Oct. 1995, pp. 1997 – 2002.

Balasuriya, B.A.A.P., Takai, M., Lam, W.C., Ura, T. & Kuroda, Y. (1997). Vision based autonomous underwater vehicle navigation: underwater cable tracking *MTS/IEEE Conference Proceedings of OCEANS '97*, Vol. 2, 6-9 Oct. 1997, pp. 1418 – 1424.

Zanoli, S.M. & Zingretti, P. (1998). Underwater imaging system to support ROV guidance, *IEEE Conference Proceedings of OCEANS '98*, Vol. 1, 28 Sept.-1 Oct. 1998, pp. 56 – 60.

Perona, P. & Malik, J. (1990). Scale-space and edge detection using anisotropic diffusion, *IEEE Transactions on Pattern Analysis and Machine Intelligence*, Vol. 12(7), July 1990, pp. 629 – 639.

Weickert, J. (2001). Applications of nonlinear diffusion in image processing and computer vision, *Proceedings of Algoritmy 2000*, Acta Math. University Comenianae Vol. LXX, 2001, pp. 33 – 50.

Blake, A. & Isard, M. (1998). Active Contour, *Springer, Berlin,* 1998.

Cootes, T., Cooper, D. Taylor, C. & Graham, J. (1995). Active shape models – their training and application, *Computer Vision and Image Understanding*, Vol. 61(1), 1995, Pages 38 – 59.

MacCormick, J. (2000). Probabilistic modelling and stochastic algorithms for visual localization and tracking. *Ph.D. thesis*, Department of Engineering Science, University of Oxford 2000.

Mobile Robots: towards New Applications

Edited by Aleksandar Lazinica

ISBN 978-3-86611-314-5

Hard cover, 600 pages

Publisher I-Tech Education and Publishing

Published online 01, December, 2006

Published in print edition December, 2006

The range of potential applications for mobile robots is enormous. It includes agricultural robotics applications, routine material transport in factories, warehouses, office buildings and hospitals, indoor and outdoor security patrols, inventory verification, hazardous material handling, hazardous site cleanup, underwater applications, and numerous military applications. This book is the result of inspirations and contributions from many researchers worldwide. It presents a collection of wide range research results of robotics scientific community. Various aspects of current research in new robotics research areas and disciplines are explored and discussed. It is divided in three main parts covering different research areas: Humanoid Robots, Human-Robot Interaction, and Special Applications. We hope that you will find a lot of useful information in this book, which will help you in performing your research or fire your interests to start performing research in some of the cutting edge research fields mentioned in the book.

InTech Europe
University Campus STeP Ri
Slavka Krautzeka 83/A
51000 Rijeka, Croatia
Phone: +385 (51) 770 447
Fax: +385 (51) 686 166
www.intechopen.com

InTech China
Unit 405, Office Block, Hotel Equatorial Shanghai
No.65, Yan An Road (West), Shanghai, 200040, China
中国上海市延安西路65号上海国际贵都大饭店办公楼405单元
Phone: +86-21-62489820
Fax: +86-21-62489821

IntechOpen